Differential effects of oleate on vascular endothelial and liver sinusoidal endothelial cells reveal its toxic features in vitro

Geng, Yana; Arroyave-Ospina, Johanna C.; Buist-Homan, Manon; Plantinga, Josée; Olinga, Peter; Reijngoud, Dirk Jan; Van Vilsteren, Frederike G.I.; Blokzijl, Hans; Kamps, Jan A.A.M.; Moshage, Han

Published in:
Journal of Nutritional Biochemistry

DOI:
10.1016/j.jnutbio.2022.109255

Publication date:
2023

Available online at www.sciencedirect.com

ScienceDirect

Journal of Nutritional Biochemistry 114 (2023) 109255

Journal of Nutritional Biochemistry

RESEARCH PAPER

Differential effects of oleate on vascular endothelial and liver sinusoidal endothelial cells reveal its toxic features *in vitro*

Yana Geng[a,c,*], Johanna C. Arroyave-Ospina[a], Manon Buist-Homan[a,b], Josée Plantinga[d], Peter Olinga[c], Dirk-Jan Reijngoud[e], Frederike G.I. Van Vilsteren[a], Hans Blokzijl[a], Jan A.A.M. Kamps[d], Han Moshage[a,b,**]

[a] Department of Gastroenterology and Hepatology, University Medical Center Groningen, University of Groningen, Groningen, The Netherlands
[b] Department of Laboratory Medicine, University Medical Center Groningen, University of Groningen, Groningen, The Netherlands
[c] Department of Pharmaceutical Technology and Biopharmacy, Groningen Research Institute of Pharmacy, University of Groningen, Groningen, The Netherlands
[d] Department of Pathology and Medical Biology, University Medical Center Groningen, University of Groningen, Groningen, The Netherlands
[e] Department of Pediatrics, University Medical Center Groningen, University of Groningen, Groningen, The Netherlands

Received 13 June 2022; received in revised form 18 November 2022; accepted 19 December 2022

Abstract

Several fatty acids, in particular saturated fatty acids like palmitic acid, cause lipotoxicity in the context of non-alcoholic fatty liver disease . Unsaturated fatty acids (*e.g.* oleic acid) protect against lipotoxicity in hepatocytes. However, the effect of oleic acid on other liver cell types, in particular liver sinusoidal endothelial cells (LSECs), is unknown. Human umbilical vein endothelial cells (HUVECs) are often used as a substitute for LSECs, however, because of the unique phenotype of LSECs, HUVECs cannot represent the same biological features as LSECs. In this study, we investigate the effects of oleate and palmitate (the sodium salts of oleic acid and palmitic acid) on primary rat LSECs in comparison to their effects on HUVECs. Oleate induces necrotic cell death in LSECs, but not in HUVECs. Necrotic cell death of LSECs can be prevented by supplementation of 2-stearoylglycerol, which promotes cellular triglyceride (TG) synthesis. Repressing TG synthesis, by knocking down DGAT1 renders HUVECs sensitive to oleate-induced necrotic death. Mechanistically, oleate causes a sharp drop of intracellular ATP level and impairs mitochondrial respiration in LSECs. The combination of oleate and palmitate reverses the toxic effect of oleate in both LSECs and HUVECs. These results indicate that oleate is toxic and its toxicity can be attenuated by stimulating TG synthesis. The toxicity of oleate is characterized by mitochondrial dysfunction and necrotic cell death. Moreover, HUVECs are not suitable as a substitute model for LSECs.

Keywords: Liver sinusoidal endothelial cells; Human umbilical vein endothelial cells; Fatty acids; Lipotoxicity; Triglycerides; Mitochondrial function.

1. Introduction

Lipid species demonstrate a high heterogeneity with regard to their biological properties. The term lipotoxicity in the context of non-alcoholic fatty liver disease/metabolic-associated fatty liver disease (NAFLD/MAFLD) describes the hepatotoxic actions of a group of lipids, particularly saturated fatty acids (*e.g.,* palmitic acid - the most abundant dietary and plasma fatty acid), which cause subcellular damage including mitochondrial damage, endoplasmic reticulum (ER) stress, oxidative stress and dysregulation of signaling pathways which may eventually lead to liver cell death [1–4]. Meanwhile, a group of non-toxic lipids, including monounsaturated fatty acids (*e.g.,* oleic acid), are generally shown to be beneficial and protective in terms of their anti-oxidative and anti-inflammatory effects. Furthermore, oleic acid was shown to protect against palmitic acid-induced cellular injury in hepatocytes [5,6] as well as in other types of cells [7,8], including vascular endothelial cells [9–12]. It is hypothesized that the protective role of oleic

Abbreviations: LSECs, liver sinusoidal endothelial cells; NAFLD, non-alcoholic fatty liver disease; MAFLD, Metabolic-associated fatty liver disease; NASH, non-alcoholic steatohepatitis; FFAs, free fatty acids; HUVECs, human umbilical vascular endothelial cells; SEM, scanning electron microscopy; HSCs, hepatic stellate cells; KCs, Kupffer cells; TG, triglyceride; OCR, oxygen consumption rate.

* Corresponding author at: Department. Gastroenterology and Hepatology, University Medical Center Groningen, Hanzeplein 1, Groningen 9713 GZ, The Netherlands.
** Corresponding author at: Depepartment. Gastroenterology and Hepatology, University Medical Center Groningen, Hanzeplein 1, Groningen 9713 GZ, The Netherlands. Tel.: +31 050 3612364; fax: +31 050 3619306.
E-mail addresses: yana.geng@rug.nl (Y. Geng), a.j.moshage@umcg.nl (H. Moshage).

https://doi.org/10.1016/j.jnutbio.2022.109255

acid is related to its proneness to be incorporated into triglycerides (TGs) [11,13]. However, contradictory results have been reported [5]. Therefore, it is still not clear how monounsaturated fatty acids like oleic acid, protect cells and whether they demonstrate similar protective effects in other types of cells, for example, liver sinusoidal endothelial cells (LSECs).

Lipid-induced cell death is mostly attributed to the induction of apoptotic cell death, which involves both intrinsic (mitochondrial/lysosomal) and extrinsic (death receptor) apoptotic pathways [2]. In recent years, it was found that lipids are also important determinants in non-apoptotic cell death, including necroptosis, ferroptosis, and pyroptosis [14,15]. Interestingly, these effects can be either toxic or protective. Under physiological conditions, oleic acid hydrolyzed from milk fat globules could induce lysosomal leakiness, which causes the release of lysosomal cathepsins leading to cell death [16,17]. On the other hand, the study from Magtanong et al. showed that oleic acid could suppress the oxidation of polyunsaturated fatty acids, preventing ferroptotic cell death [18]. Until now, there is still very limited understanding of the roles of lipids on non-apoptotic cell death.

Liver sinusoidal endothelial cells (LSECs), forming the liver sinusoids, are a special type of endothelial cells with unique phenotype. They form a discontinuous layer of endothelium, lack of basement membrane and display fenestrae organized in sieve plates, making them unique compared to other types of endothelial cells, in particular vascular endothelial cells. Functionally, LSECs also exhibit uniqueness compared to vascular endothelial cells, including their strong scavenging ability [19], immune regulatory function [20] as well as metabolic distinctness [21–23]. Importantly, LSECs have been demonstrated to be one of the first targets of lipotoxicity in NAFLD. Besides, fatty acids may modulate inflammatory chemokines in murine LSECs [24,25]. However, still very little is known about the direct effects of fatty acids on LSECs. Moreover, neither vascular endothelial cells nor commercial LSEC cell lines can properly represent primary LSECs. Therefore, in this study, we aim to investigate the differential effects of fatty acids on primary LSECs and compare their effects to vascular endothelial cells isolated from human umbilical cords (HUVECs, human umbilical vascular endothelial cells).

2. Materials and methods

2.1. Animals

Specified pathogen-free male Wistar rats (180–250 g) were purchased from Charles River Laboratories Inc. (Wilmington, MA, USA). Rats were housed under standard laboratory conditions with free access to standard laboratory chow and water. All experiments were performed according to the Dutch law on the welfare of laboratory animals and guidelines of the ethics committee of the University of Groningen for care and use of laboratory animals.

2.2. Cell isolation and culture

Primary rat LSECs were isolated by two-step collagenase perfusion [26] and centrifugation on Percoll (GE Health care, the Netherlands) density gradient. Briefly, LSECs were collected from the supernatant of the post-hepatocyte fraction, then loaded on top of 25% to 50% Percoll gradient cushions and centrifuged at 800 g for 15 min at 4°C. The interfaces between the two density cushions of 25% and 50% Percoll were collected, resuspended in preservation buffer (1% w/v BSA (Sigma-Aldrich, Zwijndrecht, the Netherlands) in HBSS solution (Thermo Fisher Scientific, Waltham, USA)) and centrifuged again. The cell pellet was resuspended and added to plastic Petri dishes (Falcon, USA) for 8 min twice to remove Kupffer cells (KCs). Subsequently, the non-attached cells were seeded on collagen-coated plates and cultured in glucose-free DMEM/RPMI 1,640 medium (1:1 v/v) supplemented with 5% heat-inactivated FCS (Fetal Calf Serum, HyClone, UK), 100 U/mL penicillin, 100 μg/mL streptomycin, 250 ng/mL fungizone (1% PSF, Lonza, Verviers, Belgium), and 40 μg/mL rat recombinant VEGF (Gibco, USA). The purity of LSECs was checked by assessing acetylated low-density lipoprotein (Dil-Ac-LDL, Thermo Fisher Scientific) uptake and assessing the mRNA expression of several specific cell markers of LSECs, hepatocytes, hepatic stellate cells (HSCs) and KCs. Experiments were performed within 48 h after isolation.

Human umbilical vein endothelial cells (HUVECs) were isolated as described before [27]. Confluent monolayers of HUVECs in passages two–three were used for experiments.

2.3. siRNA transfection

HUVECs were seeded in plates at 60% confluency. After 24 h, cells were transfected with siRNA targeting DGAT1, DGAT2 or ALLStar negative control siRNA (Qiagen, Hilden, Germany) using Lipofectamine 2,000 (Thermo Fisher Scientific) according to the manufacturer's protocol. The final concentrations of siRNAs were 6 pmol/L. Medium was refreshed after 6 h of transfection. Experiments were started 48 h after transfection and the efficiency of siRNA was assessed by qPCR.

2.4. Scanning electron microscopy

LSECs were subjected to scanning electron microscopy (SEM) to check the presence of fenestrae and sieve plates. After seeding on coverslips, LSECs were fixed with 2% glutaraldehyde (Sigma-Aldrich), and subjected to further fixation using 1% osmium tetroxide (Sigma-Aldrich) for 1 h and washed with distilled water. The dehydration process was performed in graded solutions of ethanol (30%, 50%, 70%) for 15 min each, followed by 20 min dehydration in 100% ethanol for three times and finally with tetramethylsilane (Sigma-Aldrich) for 15 min. The dried samples were coated by gold sputtering (60 s, 1.8 mA, 2.4 kV) in a Polaron SEM, SC515 coating system and imaged using SEM (Zeiss Supra 55, Germany).

2.5. Preparation of oleate-BSA and palmitate -BSA

Bovine serum albumin (BSA)-conjugated palmitate solution was prepared as described before [28]. BSA-conjugated oleate solution was prepared by conjugating 40 mmol/L oleate (Sigma-Aldrich) solution with 10% fatty acid-free BSA (Sigma-Aldrich) at 37°C. The pH was adjusted to 7.4 by addition of 1M NaOH.

2.6. Caspase 3/7 activity assay

The apoptotic cell death was measured by caspase 3/7 enzyme activity assay. After treatments, cells were washed twice with ice-cold phosphate buffered saline (PBS, Life technologies), and then added with caspase cell lysis buffer. Total cell lysates were prepared and caspase-3/7 activity was determined as described before [28].

2.7. Oil Red O staining and TG determination

Lipid droplets were visualized by Oil red O (Sigma-Aldrich) staining. HUVECs and LSECs were seeded on coverslips. After treatment, cells were rinsed with PBS and fixed with 4% (v/v) paraformaldehyde for 20 min at room temperature. After washing with distilled water, cells were washed with 60% (v/v) isopropyl alcohol and then mounted with Oil Red O solution (Sigma-Aldrich) dissolved in isopropyl alcohol. Then cells were rinsed in distilled water and 60% (v/v) isopropyl alcohol again, counterstained with hematoxylin, rinsed with tap water and sealed in glycerin gelatin. The coverslips were scanned with a digital slide scanner (Hamamatsu, Japan) and the lipid droplets were identified by red staining.

To quantify the lipid accumulation, intracellular TG level was measured using a TG measurement kit (Abcam, UK) following the guidelines provided by the company. The number of TGs was normalized to the number of cells.

2.8. Sytox Green nuclear staining

The necrotic cell death was determined by Sytox Green nuclear staining. Briefly, after treatments, cells were incubated with Sytox green nucleic acid dye (Invitrogen) for 15 min as described before [29]. Fluorescent nuclei were visualized using a Leica DMI6000 at 450–490 nm.

2.9. Lactate dehydrogenase (LDH) release assay

Necrosis was quantified by lactate dehydrogenase (LDH) release measurement, as described by Woudenberg-Vrenken et al. [30]. Briefly, the LDH release was calculated as the percentage of the activity of LDH released in the medium *versus* the total LDH activity (in both the medium and cell lysates). LDH activity was measured spectrophotometrically at 340 nm using an Epoch2 microplate reader (Bio-Tek Instruments, Inc., Winooski, VT, USA).

2.10. Luciferase-based ATP measurement

Luminescent ATP detection assay kit (Promega, USA) was used to measure intracellular ATP level. Cells were seeded in black 96 well plates. Cellular ATP level was measured as described before [29] and following the instructions provided by the company. Luminescence from luciferase activity was measured and recorded using a Synergy H4 microplate fluorescent reader (Bio-Tek).

2.11. Western-blot analysis

To evaluate the expression of specific proteins, the total cell lysate was subjected to Western-blot as described by Woudenberg-Vrenken et al [26]. Proteins were detected using the following antibodies: p-JNK (Thr183/Tyr185) (Cell Signaling Technology, Leiden, the Netherlands), JNK (Cell Signaling Technology), β-actin (Cell Signaling Technology), PARP (Cell Signaling Technology), cleaved-caspase 3 (Cell Signaling Technology). The goat anti-rabbit horseradish peroxidase-labeled secondary antibody (Agilent, Santa Clara, CA, USA) was used to visualize immunoreactive bands, which were imaged with ChemiDoc System (Bio-rad, the Netherlands). The expression of proteins was quantified from the immunoblots by densitometry from 3 to 5 independent experiments with ImageJ.

2.12. RNA isolation and quantitative polymerase chain reaction

Total RNA was isolated using Tri-reagent (Sigma-Aldrich) according to the manufacturer's instruction. The RNA quantity and quality were measured with the Nanodrop spectrophotometer (Thermo Fisher Scientific). Reverse transcription was performed on 2.5 μg RNA. Quantitative real-time PCR was performed with the 7900HT Fast Real-time System (Applied Biosystems, Waltham, MA, USA) using the TaqMan protocol or SYBR Green protocol. mRNA levels were normalized to *18S* or *GAPDH*, and then further normalized to the expression of control groups. The primers and probes are shown in Supplemental Table 1.

2.13. Monitoring of mitochondrial respiration by Seahorse system

The oxygen consumption rate (OCR) was measured by the Seahorse system (Billerica, MA, USA). Freshly isolated LSECs were seeded in XF24 cell culture plates coated with collagen. After exposure to oleate and/or palmitate, cells were washed with PBS and XF assay medium supplemented with 1 mmol/L sodium pyruvate and incubated in a non-CO_2 incubator at 37°C for 60 min. OCR was measured with XF24 Extracellular Flux Analyzer (Seahorse Bioscience) using manufacturer recommended protocols. After normalizing to protein concentration, basal respiration, proton leak and coupling efficiency were calculated. Specifically, the basal respiration is calculated without glucose and all rates were corrected for non-mitochondrial OCR as indicated before [28].

2.14. BODIPY 493/503 staining

To visualize lipid droplets, BODIPY 493/503 probe (Thermo Fisher Scientific) was used, according to protocol previously described [31]. Briefly, cells were seeded on coverslips and after treatment were washed with PBS. After that cells were stained with BODIPY working solution (2 μmol/L) for 15–20 min and then washed with PBS and fixed with 4% paraformaldehyde. Coverslips were mounted in DAPI antifade mounting medium (Vectashield, Vector Laboratories, Gdynia, Poland) and protected from light, and then images were visualized in the fluorescent microscope (Leica, Wetzlar, Germany) and analyzed using ImageJ.

2.15. Statistical analysis

All results are presented as the mean of at least 3 independent experiments ± S.D. For each experiment, statistical analyses were performed using Kruskal–Wallis test, followed by Dunn's multiple comparison tests or using Mann Whitney test; $p<0.05$ was considered as statistically significant.

3. Results

3.1. Oleate protects against palmitate-induced apoptotic cell death and endothelial dysfunction in HUVECs, but induces necrosis in LSECs

In HUVECs, palmitate time- and concentration-dependently induces caspase 3/7 activity (Supplementary Fig. 1A and 1B), indicating a stimulated apoptotic cell death. The caspase 3/7 activity peaks around 12 h and shows a significant increase at 0.5 mmol/L ($p<0.001$). Therefore, 0.5 mmol/L palmitate and 12 h treatment was used in all experiments, unless otherwise indicated. On the other hand, oleate did not induce caspase 3/7 activity and concentration-dependently rescued palmitate-induced apoptotic cell death, which significantly reduced caspase 3/7 at 0.25 mmol/L (Supplementary Fig. 1C, $p<0.05$). The effects of oleate and palmitate were further investigated by Western-blot and real-time PCR. Oleate (0.25 mmol/L) showed no toxicity in HUVECs, demonstrated by a lack of a significant increase of p-JNK/JNK, cleaved-caspase 3/β-actin and cleaved-PARP/PARP ($p>0.05$, Fig. 1A) and no significant changes of the expression of adhesion molecules (*ICAM-1, VCAM-1, e-SELECTIN*), inflammatory genes (*COX2*) and vasoprotective gene (e*NOS*) ($p>0.05$, Fig. 1B). Palmitate (0.5 mmol/L) significantly increased the levels of apoptotic proteins (p-JNK/JNK, cleaved-caspase 3/β-actin and cleaved-PARP/PARP) ($p<0.05$, Fig. 1A) and significantly increased expression of *ICAM-1, VCAM-1, e-SELECTIN, COX2* and decreased expression of e*NOS* ($p<0.01$, Fig. 1B). However, the combination of oleate and palmitate exhibited no toxicity as demonstrated by the lack of apoptotic cell death and no changes in gene expression (Fig. 1A and 1B).

Next, we compared the effects of oleate and palmitate on HUVECs to those in LSECs. Primary rat LSECs were isolated from Wistar rats (180–250g) and seeded on collagen-coated plates. A light microscope picture is shown in Supplementary Fig. 2A. After 2 h of attachment, LSECs were incubated with Dil-Ac-LDL (10 μg/mL) to check the confluency and purity. This result shows that more than 95% of the cells were positive for Dil-Ac-LDL staining (Supplementary Fig. 2B). Scanning electron microscopy (SEM) images were taken to check the presence of fenestrae, which is the gold standard for confirming the identity of LSECs (Supplementary Fig. 2 C). To further assess the contamination by other types of liver cells (hepatocytes, HSCs and KCs), the mRNA expression of several cell markers (*eNOS, STAB2, ALB, ACTA2, CD68*) were measured. Results indicate low contamination of our LSEC preparations by hepatocytes, HSCs and KCs (Supplementary Fig. 2D).

Freshly isolated primary rat LSECs were challenged with oleate (0.15 mmol/L, 0.25 mmol/L) and/or palmitate (0.5 mmol/L). The images of the cells were taken by IncuCyte® Live-cell imaging system every 2 h. As shown in Supplementary Fig. 3, oleate at 0.15 mmol/L did not cause morphological changes, however, oleate at 0.25 mmol/L caused a rapid cell crenation, blister formation on plasma membrane and condensation of the nucleus, starting 2 h after oleate addition. Palmitate and the combination of oleate and palmitate did not lead to morphological changes either (Supplementary Fig. 3). The complete videos of 16 h of incubation are enclosed in supplementary files. Therefore, to study the toxicity of oleate in LSECs and consistent to the concentration of oleate used in HUVECs, 0.25 mmol/L of oleate was used in LSECs experiments. Besides the morphological changes, as shown in Fig. 1C, oleate (0.25 mmol/L) also induced Sytox Green nuclei staining (Fig. 1D) and a significant increase of LDH release ($p<0.01$, Fig. 1E), which indicate that oleate induces necrosis in LSECs. However, the combination of oleate and palmitate did not induce necrotic cell death in LSECs (Fig. 1C–E). On the other hand, similar to the observations in HUVECs, palmitate induced apoptotic cell death in LSECs, shown by the significantly increased levels of p-JNK/JNK, cleaved-caspase 3 (especially the fully matured p17 fragment)/β-actin and cleaved-PARP/PARP ($p<0.05$, Fig. 1F), assessed at 16 h. However, the combination of oleate and palmitate also did not induce apoptotic cell death (Fig. 1F). Of note, since oleate caused rapid cell rupture, it was not possible to harvest cells after exposure to oleate at 16 h.

3.2. The lack of toxicity after oleate and/or palmitate treatment correlates with lipid droplet formation and increased TG synthesis in both HUVECs and LSECs

Since TGs are considered to be a type of inert, non-toxic lipids stored in lipid droplets [13,32,33], we checked lipid droplet formation and cellular TG synthesis in HUVECs and LSECs. Noticeably, in HUVECs, both oleate and palmitate caused intracellular lipid accumulation, whereas palmitate-induced lipids are morphologically different in oil red O staining. The combination of oleate and palmitate promoted the formation of lipid droplets in both HUVECs and LSECs (Fig. 2A and 2D), and increased the cellular TG levels

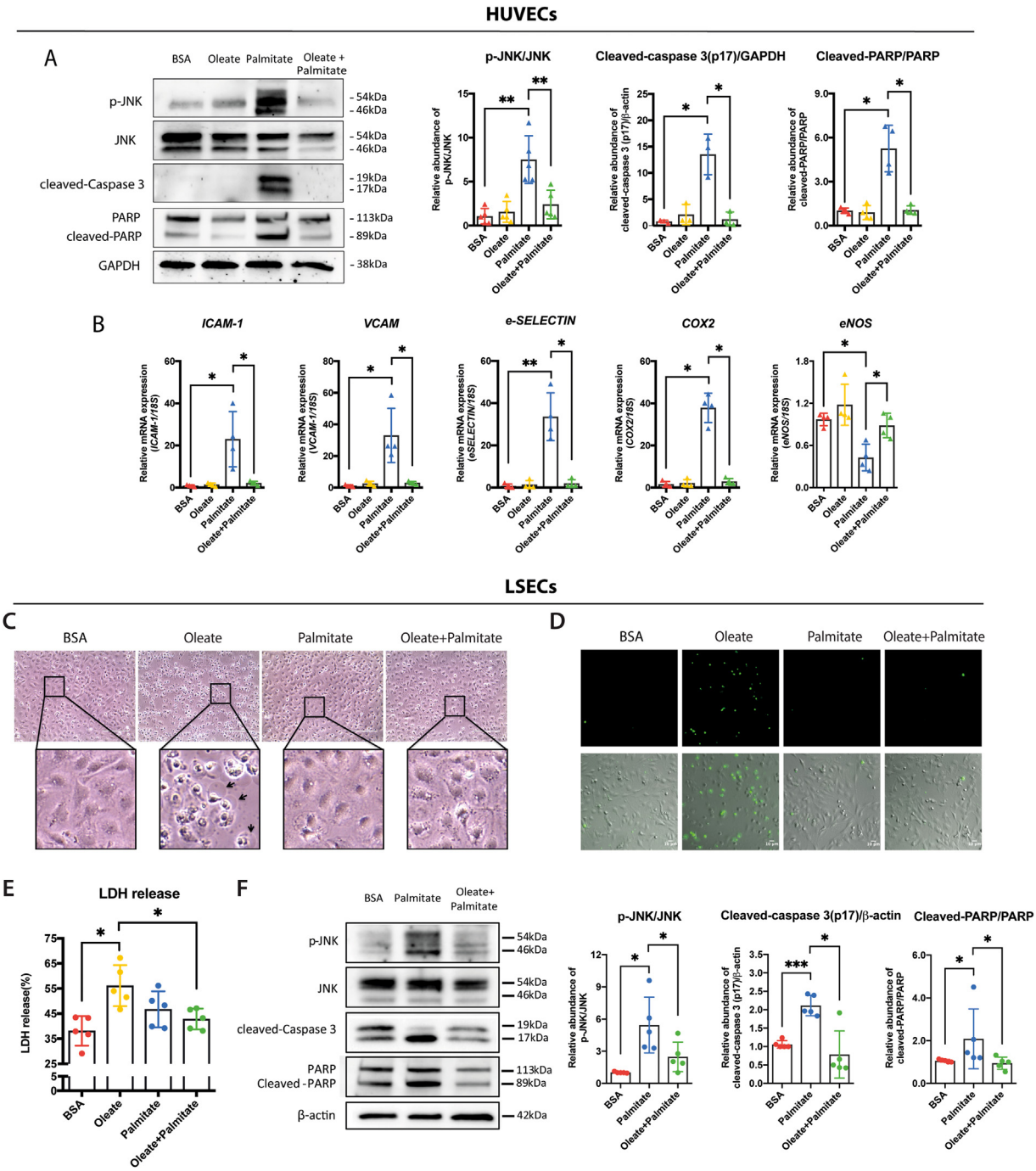

Fig. 1. Oleate protects against palmitate-induced apoptosis and endothelial dysfunction in HUVECs, but induces necrosis in LSECs. (A–B) HUVECs were treated with oleate (0.25 mmol/L) and/or palmitate (0.5 mmol/L) for 12 h. (A) Protein levels of p-JNK, JNK, cleaved-caspase 3, PARP, and β-actin were assessed via Western blot and quantified from the immunoblots by densitometry from 3 to 5 independent experiments with ImageJ. (B) mRNA expressions of *ICAM-1, VCAM-1, e-SELECTIN, COX2,* and *eNOS* was measured by real-time quantitative PCR. (C–E) Freshly isolated LSECs were treated with oleate (0.25 mmol/L) and/or palmitate (0.5 mmol/L). (C) Representative light microscopy pictures were taken after 8 h of treatment. Scale bar: 100 μm. (D) Plasma membrane rupture indicative of necrotic cell death is demonstrated by Sytox Green staining. Scale bar: 10 μm. (E) Necrosis was quantified by measuring LDH release shown as the percentage of total LDH released in the medium after 24 h treatment. (F) LSECs were harvested after 16 h of treatment with palmitate or the combination of oleate and palmitate. Protein levels of p-JNK, JNK, cleaved-caspase 3, PARP and β-actin were assessed via Western blot and quantified from the immunoblots by densitometry from 3 to 5 independent experiments with ImageJ. Data are shown as mean ± S.D. ($n \geq 3$). * Indicates $p<0.05$, ** indicates $p<0.01$, ns indicates $p>0.05$.

($p<0.05$, Fig. 2B and 2E). Moreover, oleate increased the expression of *DGAT1* in HUVECs ($p=0.056$), whereas the combination of oleate and palmitate significantly increased the expression of both *DGAT1* and *DGAT2* ($p<0.05$), but not *GPAT* ($p>0.05$) in LSECs (Fig. 2C and 2F). Of note, the expression of *DGAT1* is around 100 times higher than *DGAT2* in both HUVECs and LSECs (Fig. 2C and 2F). In addition, to check whether oleate induces lipid droplets in LSECs, we stained cells with BODIPY 493/503 at earlier time points (1–6 h) after incubations with oleate, palmitate or oleate + palmitate (Supplementary Fig. 4). There are few of lipid droplets in LSECs at 4

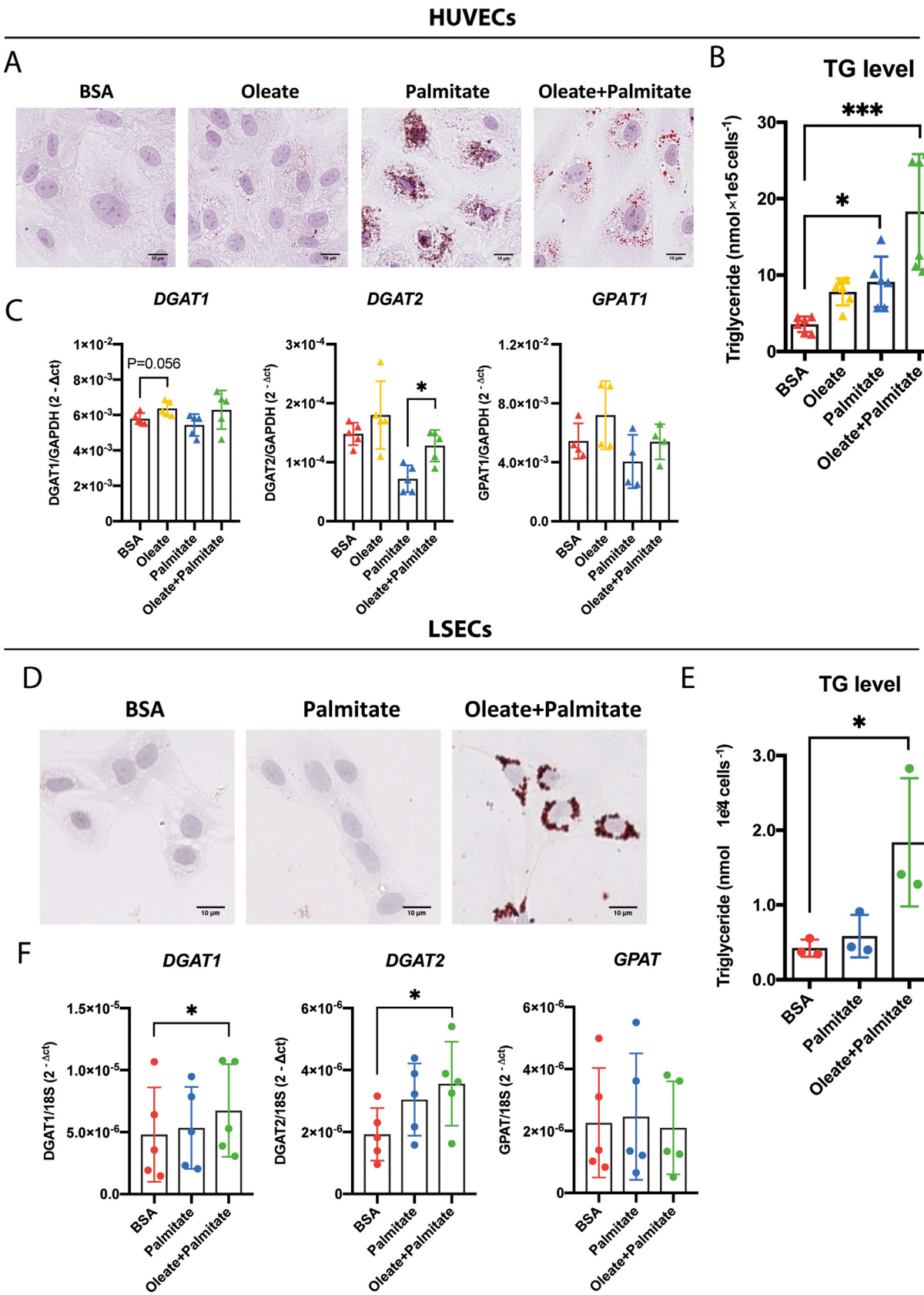

Fig. 2. The lack of toxicity after oleate and/or palmitate treatment correlates with lipid droplet formation and increased TG synthesis in both HUVECs and LSECs. HUVECs and freshly isolated LSECs were treated with oleate (0.25 mmol/L) and/or palmitate (0.5 mmol/L) for 12 h. (A and D) The formation of lipid droplets was assessed via oil red O staining. Scale bar: 10 μm. (B and E) Cellular TG level was quantified and normalized to cell number. (C and F) mRNA expressions of *DGAT1*, *DGAT2* and *GPAT1* was measured by real-time quantitative PCR. Data are shown as mean ± S.D. ($n \geq 3$). * Indicates $p<0.05$, ns indicates $p>0.05$.

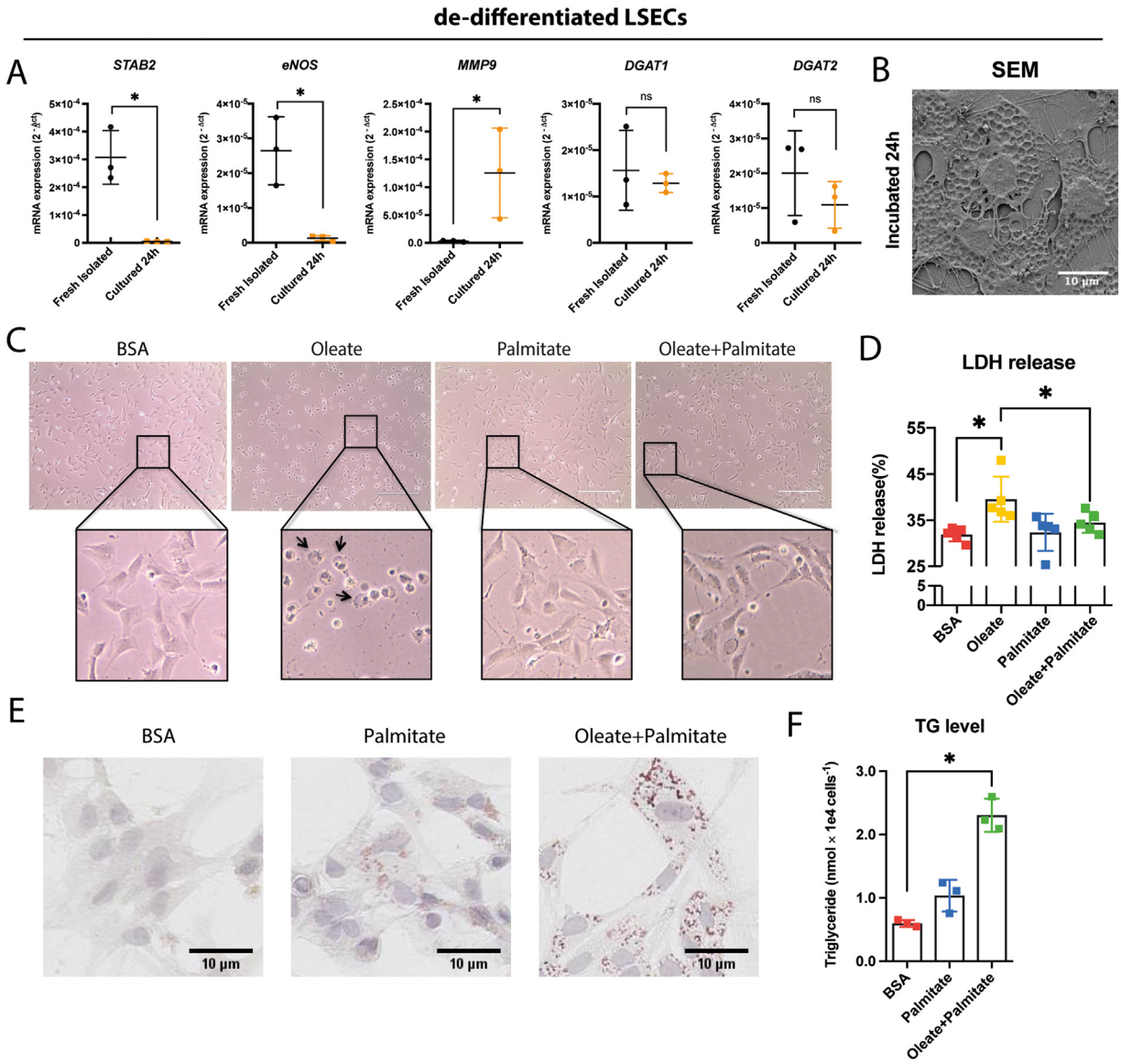

Fig. 3. In de-differentiated LSECs, oleate but not the combination of oleate and palmitate induces necrotic cell death. Freshly isolated LSECs were kept in culture for 24 h to obtain the de-differentiated phenotype. (A) RNA was isolated from both freshly isolated LSECs and de-differentiated LSECs, mRNA expressions of *STAB2, eNOS* and *MMP9* were evaluated by real-time quantitative PCR. (B) Fenestrae were assessed by scanning electron microscope (SEM). Scale bar: 10 μm. (C) De-differentiated LSECs were treated with oleate (0.25 mmol/L) and/or palmitate (0.5 mmol/L). Representative light microscopy pictures were taken after 12 h of treatment. (D) Necrosis was quantified by measuring LDH release and shown as the percentage of total LDH released in the medium after 24 h treatment. (E) The formation of lipid droplets was assessed via oil red O staining. Scale bar: 10 μm. (F) Cellular TG level was quantified and normalized to the cell numbers. Data are shown as mean ± S.D. ($n \geq 3$). * and # indicate $p<0.05$, ** indicates $p<0.01$, ns indicates $p>0.05$.

h, however it is much less than that in the non-toxic condition (oleate + palmitate).

3.3. In dedifferentiated LSECs, oleate but not the combination of oleate and palmitate induces necrotic cell death

Since oleate demonstrates cell type specific effects and the biological and physiological features and functions of LSECs change greatly with regard to its differentiation states, we checked whether the toxic effect of oleate in LSECs is dependent on the differentiation state of LSECs. Freshly isolated and early cultured LSECs represent the differentiated phenotype. However, upon prolonged culture and in diseased liver, LSECs dedifferentiate and undergo capillarization, as demonstrated by the loss of fenestrae and the development of an organized basement membrane *in vivo* and changes in the expression of function-related genes, like *STAB2, eNOS* and *MMP9* [34–36]. Therefore, we kept freshly isolated LSECs in culture for 24 h, allowing the LSECs to exhibit their dedifferentiated phenotype demonstrated by reduced *STAB2* and e*NOS* expression and increased *MMP9* expression, whereas the mRNA expressions of *DGAT1* and *DGAT2* showed no significant changes (Fig. 3A). In addition, the cultured LSECs showed a loss of fenestration after 24 h (Fig. 3B). In dedifferentiated LSECs, oleate (0.25 mmol/L) still induced necrotic cell death, as shown by the morphological changes and significantly increased LDH release ($p<0.01$, Fig. 3C and 3D). The combination of oleate and palmitate (0.5 mmol/L) was not toxic and promoted lipid droplet formation and significantly increased cellular TG synthesis (Fig. 3E and 3F). These results indicate that the toxic effects of fatty acids are not specific for the differentiated phenotype of LSECs.

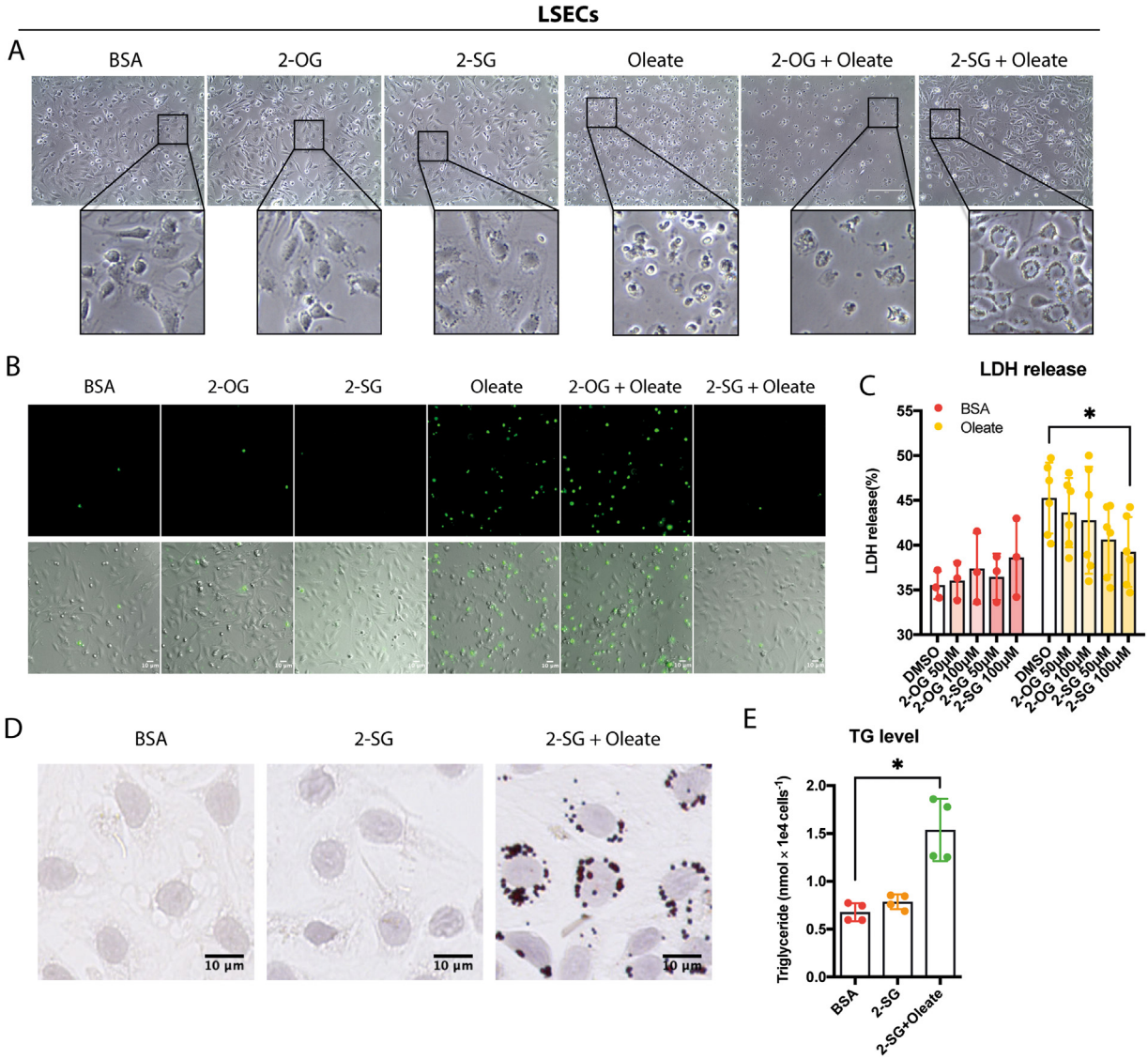

Fig. 4. Supplementation of 2-Stearoyl glycerol (2-SG) alleviates oleate-induced cell death and promotes lipid droplet formation in LSECs. Freshly isolated LSECs were pre-treated with 2-OG (2-oleoylglycerol, 100 μmol/L) or 2-SG (2-stearoylglycerol, 100 μmol/L) for 1 h, and then supplemented with oleate (0.25 mmol/L). (A) Representative light microscopy pictures were taken after 8 h of treatment. Scale bar: 100 μm. (B) Necrotic cell death was indicated by Sytox Green staining. Scale bar: 10 μm. (C) Necrosis was quantified by measuring LDH release shown as the percentage of total LDH released in the medium after 16 h treatment. (D) The formation of lipid droplet was assessed via oil red O staining. Scale bar: 10 μm. (E) Cellular TG level was quantified and normalized to cell number. Data are shown as mean ± S.D. ($n \geq 3$). * Indicates $p < 0.05$, ns indicates $p > 0.05$.

3.4. Supplementation of 2-Stearoylglycerol alleviates oleate-induced cell death and promotes lipid droplet formation in LSECs

To investigate whether TG synthesis and lipid droplet formation are related to the toxicity of FFAs, we stimulated the biosynthesis of TGs by supplementing LSECs with exogenous monoacylglycerol. The monoacylglycerol pathway is one of the important routes in the biosynthesis of TGs. After seeding, 2-oleoylglycerol (2-OG, 50 μmol/L and 100 μmol/L) and 2-stearoylglycerol (2-SG, 50 μmol/L and 100 μmol/L) were supplemented to LSECs 1 h before addition of oleate (0.25 mmol/L). As shown in Fig. 4A and 4B, 2-OG and 2-SG did not cause morphological changes nor cell death in LSECs. Importantly, 2-SG, but not 2-OG, protected against oleate-induced cell death. The protective effects were quantified by LDH release assay, which shows that 2-SG (100 μmol/L) significantly reduced oleate-induced LDH release ($p < 0.05$, Fig. 4C). Furthermore, the supplementation of 2-SG promoted the formation of lipid droplets and significantly increased the synthesis of TGs ($p < 0.05$) (Fig. 4D and 4E).

3.5. Knockdown of DGAT1 induces the necrotic effect of oleate, but not oleate + palmitate, in HUVECs

To further investigate whether the "non-toxic" feature of oleate in HUVECs is dependent on TG synthesis, we impeded the synthesis of TG by knocking down DGAT1 and/or DGAT2, the rate-limiting enzymes in the synthesis of TG, using siRNA. After 48 h siRNA transfection, the knockdown efficiency was assessed by mRNA expressions of *DGAT1* and *DGAT2*. The results show that the mRNA expression of *DGAT1* was reduced by 88.34 ± 7.14% and *DGAT2* by 50.36 ± 20.26% (Fig. 5A). Importantly, oleate induced necrosis in siDGAT1 knockdown cells. It significantly increased LDH release when HUVECs were transfected with siDGAT1 or siDGAT1 and siDGAT2 ($p < 0.05$, Fig. 5B). Meanwhile, DGAT2 knockdown did

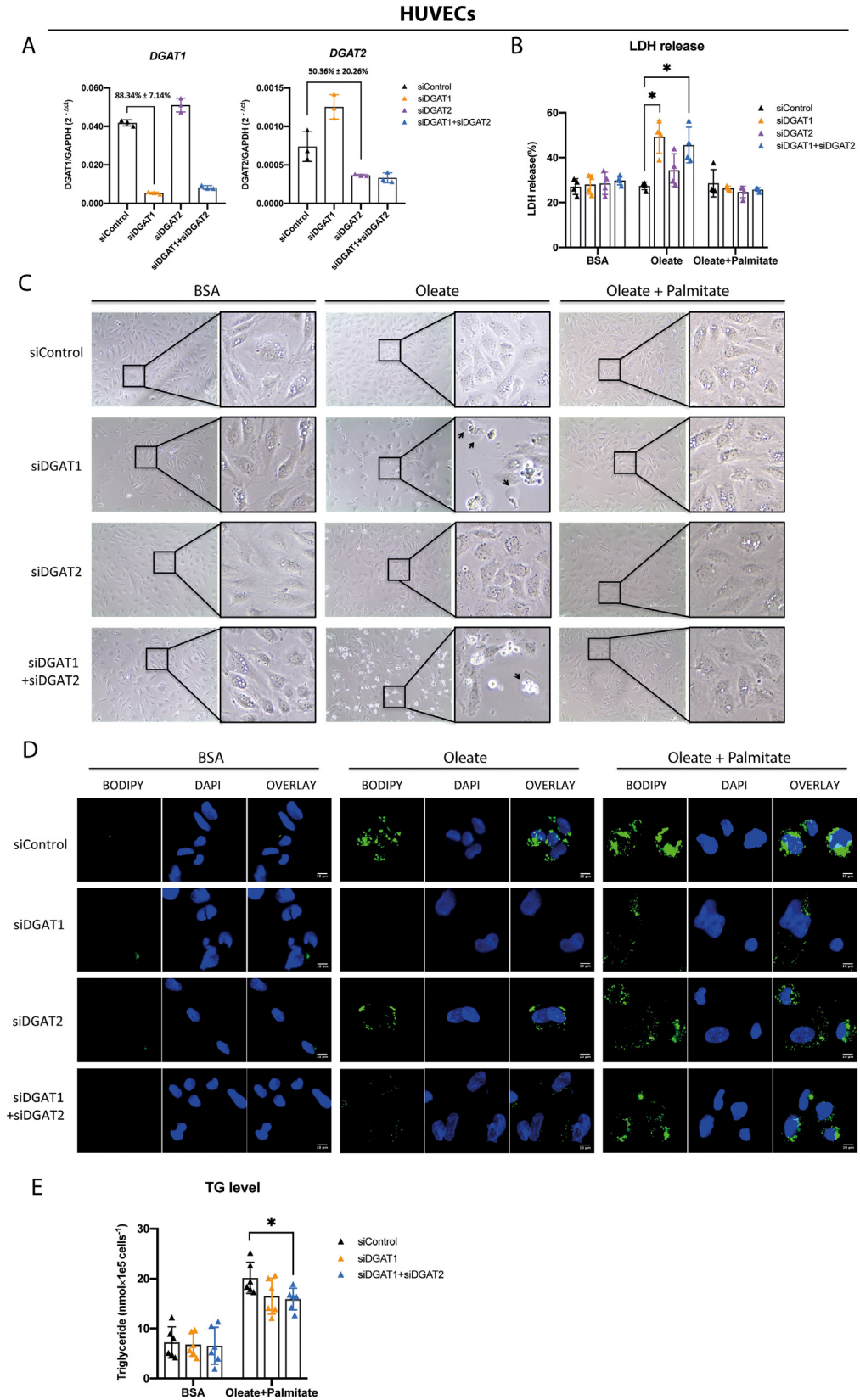

Fig. 5. Knockdown of DGAT1, but not DGAT2, unveils the necrotic effect of oleate in HUVECs. HUVECs were transfected with siControl, siDGAT1 and/or siDGAT2 for 48 h, then treated with oleate (0.25 mmol/L) or oleate (0.25 mmol/L) and palmitate (0.5 mmol/L). (A) After transfection, mRNA expressions of *DGAT1* and *DGAT2* were measured by real-time quantitative PCR. (B) After 24 h treatment of oleate and palmitate, necrosis was quantified by measuring LDH release shown as the percentage of total LDH released in the medium. (C) Representative light microscopy pictures were taken after 6 h of treatment. Scale bar: 100 μm. (D) The formation of lipid droplet was assessed via oil red O staining after 24 h treatment. Scale bar: 10 μm. (E) Cellular TG level was quantified and normalized to cell number. Data are shown as mean ± S.D. ($n \geq 3$). * Indicates $p<0.05$.

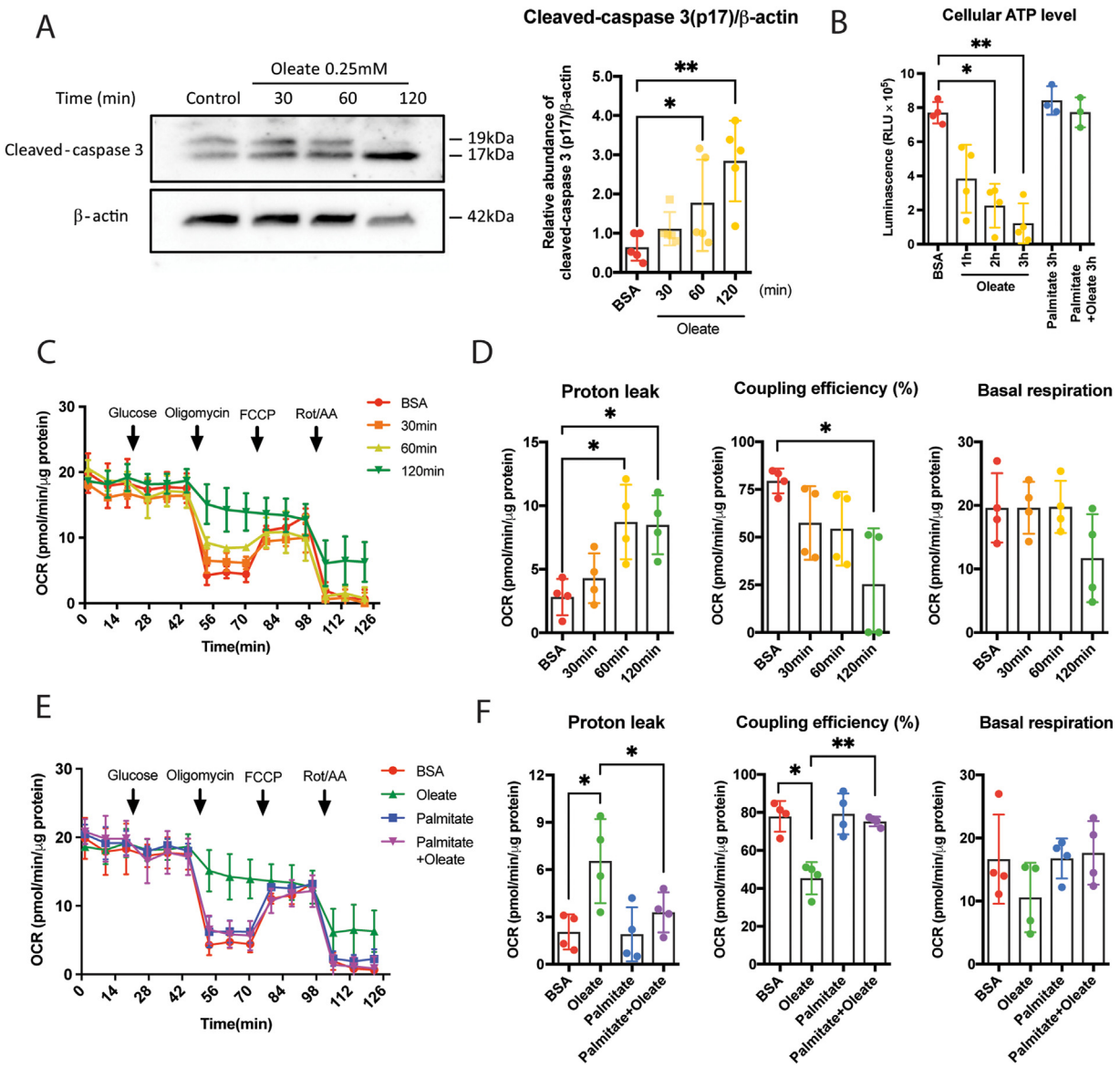

Fig. 6. Oleate causes mitochondrial dysfunction in LSECs. Freshly isolated LSECs were treated with oleate (0.25 mmol/L) and/or palmitate (0.5 mmol/L) for the time indicated in each experiment. (A) Protein levels of cleaved-caspase 3 and β-actin were assessed via Western-blot. (B) Cellular ATP level was measured via a Luciferase-based assay. (C and E) Real-time OCR was measured using the XF24 analyzer and normalized to total protein. Injections include glucose (5 mmol/L), oligomycin (1 μmol/L), FCCP (Carbonyl cyanide-4-(trifluoromethoxy)phenylhydrazone, 0.75 μmol/L) and rotenone (1 μmol/L)/AA (Antimycin, 1 μmol/L) sequentially. (D and F) Proton leak, coupling efficiency and basal respiration were calculated to illustrate the changes in metabolic profile. Data are shown as mean ± S.D. ($n \geq 3$). * indicates $p<0.05$, ** indicates $p<0.01$, ns indicates $p>0.05$.

not potentiate oleate-induced cell death. Moreover, morphologically, in siDGAT1 knockdown cells, HUVECs also exhibit blisters on plasma membranes after oleate treatment (Fig. 5C). Of note, the combination of oleate and palmitate did not cause cell death in siDGAT1 and/or siDGAT2 knockdown cells, which was again accompanied by lipid droplet formation and increased TG synthesis, although the TG level was decreased after knocking down DGAT1 and DGAT2 ($p<0.05$, Fig. 5D and 5E).

3.6. Oleate causes mitochondrial dysfunction in LSECs

Although we have shown that oleate mainly induces necrosis in LSECs, we also observed a significantly increased level of cleaved-caspase 3 in the first 2 h of oleate treatment ($p<0.05$, Fig. 6A), which indicates early-stage apoptosis. Meanwhile, as shown in Fig. 6B, oleate caused a sharp drop of intracellular ATP level resulting in more than 80% loss of cellular ATP after 3 h ($p<0.01$). The reduced ATP level may favor necrotic cell death and abrogate the progression of apoptotic cell death even with an increased expression of cleaved-caspase 3, because apoptosis is an ATP-dependent process.

Because oleate induced a sharp drop of cellular ATP level, the mitochondrial respiration was investigated via the Seahorse analyzer. Freshly isolated LSECs were seeded in Seahorse 24XF culture plate and then treated with oleate and/or palmitate for 2 h or with oleate alone for several time intervals. Seahorse results show that oleate disrupted mitochondrial respiration in a time-dependent manner, demonstrated by increased proton leak, decreased coupling efficiency, but unchanged basal respiration (Fig. 6C and 6D). On the other hand, neither palmitate nor the combination of oleate and palmitate caused significant changes in mitochondrial respiration (Fig. 6E and 6F). These results imply that oleate may func-

tion as an uncoupler of the mitochondrial respiration chain in LSECs.

4. Discussion

In this study, we show that LSECs and HUVECs exhibit differences in response to oleate. In HUVECs, oleate is not toxic and protected against palmitate-induced cellular dysfunction and apoptosis. However, in LSECs, oleate causes rapid necrotic cell death, whereas palmitate causes apoptotic cell death. The combination of oleate and palmitate is non-toxic. Importantly, the non-toxic conditions in both types of cells are consistently correlated with increased TG synthesis and the formation of lipid droplets. Furthermore, promoting the formation of TGs alleviated oleate-induced cell death in LSECs, whereas inhibiting TG synthesis provokes oleate-induced cell death in HUVECs. These results indicate that the effect of oleate is cell type specific and may related to the cellular ability of TG synthesis. Moreover, the toxic mechanisms of oleate are different from those of palmitate, in that it causes severe mitochondrial dysfunction which leads to necrotic cell death rather than apoptotic cell death as occurs with palmitate.

Oleate is generally believed to be one of the beneficial fatty acids and it has been shown to possess anti-inflammatory, antioxidant and cytoprotective properties [9,37–40]. However, our current study indicates that oleate is in fact extremely toxic for LSECs. Previously, toxicity of oleic acid was also observed in human β-cells [41] and in HSCs [42], although both of these studies used higher concentrations of oleic acid (0.5 mmol/L and 1.0 mmol/L respectively) and the mechanisms were not explained. In our present study, we show that a relatively low concentration of oleate (0.25 mmol/L) directly caused necrotic cell death in LSECs as well as in HUVECs with DGAT1 silencing, indicating that oleate is in fact a toxic fatty acid, unless it is incorporated into TGs.

Mechanistically, the “protective” actions of oleate were suggested to be related to TG synthesis [38]. This hypothesis was supported by the study from Listenberger et al. showing that oleate induced cell death in DGAT1 knockout mouse embryonic fibroblasts, which have impaired TG synthesis capacity [13]. However, it was still a matter of debate whether the increased TG synthesis and/or lipid droplet biogenesis is the protective mechanism against lipotoxicity [42]. One study in hepatocytes showed that oleate protected against palmitate-induced lipotoxicity in DGAT1 and DGAT2 double knockdown cells, by reducing the cellular uptake and esterification of palmitate [5]. Another study in pancreatic β-cells showed that the lipid droplet formation is not essential for the protection against lipotoxicity by knocking down lipid droplet proteins - perilipin 1 and 2 [42]. In the present study, we show that the toxicity of oleate depends on its ability to be incorporated into TGs. Moreover, it is likely that the rate of incorporation of fatty acids into TGs limits this rescuing mechanism for oleate. The three acyl groups in TG are usually different with regard to their saturation. Therefore, oleate is more readily incorporated in 2-SG rather than 2-OG. This may explain why the supplementation of 2-OG did not prevent oleate-induced cell death (Fig 3A and 3B). On the other hand, after knocking down DGAT1 and DGAT2, HUVECs could still form a significant amount of TGs with the addition of oleate and palmitate (Fig 4D and 4E). This might due to the remaining DGAT1/2 activities or might be another TG synthesis pathway is involved when both oleate and palmitate are present. Additionally, it was reported that in NAFLD the lipid droplet content in LSECs contains more unsaturated lipids concomitant with an increased expression of stearylo-CoA desaturase 1 [43]. This observation provides *in vivo* indication that LSECs are liable to unsaturated fatty acid-induced damage and tend to incorporate it in lipid droplet.

Contrary to the commonly observed apoptotic cell death induced by toxic fatty acids, in the present study we showed that oleate caused rapid necrotic cell death, which is characterized by blisters formed on the plasma membrane. Furthermore, the toxic actions of oleate are related to the dysfunction of mitochondria and subsequent ATP depletion. Of note, oleate also caused the activation of caspase 3 within the first 2 h, but because of the low cellular ATP level, apoptosis is abrogated and is not the main mode of cell death that leads to cell demise. As shown in the Seahorse results (Fig. 5C–F), oleate time-dependently caused the dysfunction of mitochondrial respiration. Specifically, the changes in the OCR pattern imply that oleate might work as an uncoupler, increasing proton leak, decreasing coupling efficiency but not changing the basal respiration. More detailed investigations and confirmation of oleate as a mitochondrial uncoupler are needed. In addition, since the blisters on plasma membrane are also an important morphological feature of pyroptosis [44–46], we also checked several pyroptotic markers, including caspase 1, GSDMD and IL-1β. However, we did not observe indications of pyroptotic cell death upon oleate treatment (data not shown). Therefore, more studies are needed to examine whether the blisters induced by oleate are related to other modes of cell death.

In summary, HUVECs and LSECs respond to oleate differentially. Oleate is not toxic in HUVECs but induces necrotic cell death in LSECs, which is related to the damage of mitochondria. The toxic actions of oleate can be abrogated when incorporated into TG. Moreover, palmitate induces apoptotic cell death and the combination of oleate and palmitate promotes their incorporation into TGs. Overall, although many studies looked into the interactions between lipids and vascular endothelial cells [47,48], given the uniqueness of LSECs, further studies are needed to better understand the metabolic regulations of lipids in LSECs which may provide a new insight in the pathogenesis and therapeutic strategies in NAFLD.

Acknowledgments

This project is financially supported by the China Scholarship Council (File No. 201506210062) (Y.Geng.); and Colciencias International Scholarship Program, Minciencias Colombia (783-2017) (J.C.Arroyave-Ospina).

Declaration of competing interest

The authors acknowledge no conflicts of interest with this study.

Supplementary materials

Supplementary material associated with this article can be found, in the online version, at doi:10.1016/j.jnutbio.2022.109255.

CRediT authorship contribution statement

Yana Geng: Conceptualization, Investigation, Methodology, Formal analysis, Data curation, Writing – original draft. **Johanna C. Arroyave-Ospina:** Investigation, Methodology, Writing – review & editing. **Manon Buist-Homan:** Investigation, Methodology. **Josée Plantinga:** Investigation, Methodology. **Peter Olinga:** Resources. **Dirk-Jan Reijngoud:** Methodology. **Frederike G.I. Van Vilsteren:** Writing – review & editing. **Hans Blokzijl:** Writing – review & editing, Funding acquisition, Supervision. **Jan A.A.M. Kamps:** Resources, Writing – review & editing, Supervision. **Han Moshage:** Conceptualization, Funding acquisition, Supervision, Writing – review & editing, Project administration.

References

[1] Arroyave-Ospina JC, Wu Z, Geng Y, Moshage H. Role of oxidative stress in the pathogenesis of non-alcoholic fatty liver disease: implications for prevention and therapy. Antioxidants (Basel) 2021;10:1–25.
[2] Geng Y, Faber KN, de Meijer VE, Blokzijl H, Moshage H. How does hepatic lipid accumulation lead to lipotoxicity in non-alcoholic fatty liver disease? Hepatol Int 2021;15:21–35.
[3] Leamy AK, Egnatchik RA, Young JD. Molecular mechanisms and the role of saturated fatty acids in the progression of non-alcoholic fatty liver disease. Prog Lipid Res 2013;52:165–74.
[4] Musso G, Cassader M, Paschetta E, Gambino R. Bioactive lipid species and metabolic pathways in progression and resolution of nonalcoholic steatohepatitis. Gastroenterology 2018;155:282–302 e8.
[5] Leamy AK, Hasenour CM, Egnatchik RA, Trenary IA, Yao CH, Patti GJ, et al. Knockdown of triglyceride synthesis does not enhance palmitate lipotoxicity or prevent oleate-mediated rescue in rat hepatocytes. Biochim Biophys Acta 2016;1861:1005–14.
[6] Ricchi M, Odoardi MR, Carulli L, Anzivino C, Ballestri S, Pinetti A, et al. Differential effect of oleic and palmitic acid on lipid accumulation and apoptosis in cultured hepatocytes. J Gastroenterol Hepatol 2009;24:830–40.
[7] Chen X, Li L, Liu X, Luo R, Liao G, Li L, et al. Oleic acid protects saturated fatty acid mediated lipotoxicity in hepatocytes and rat of non-alcoholic steatohepatitis. Life Sci 2018;203:291–304.
[8] Haffar T, Berube-Simard F, Bousette N. Impaired fatty acid oxidation as a cause for lipotoxicity in cardiomyocytes. Biochem Biophys Res Commun 2015;468:73–8.
[9] Ciapaite J, van Bezu J, van Eikenhorst G, Bakker SJ, Teerlink T, Diamant M, et al. Palmitate and oleate have distinct effects on the inflammatory phenotype of human endothelial cells. Biochim Biophys Acta 2007;1771:147–54.
[10] Lee DM, Sevits KJ, Battson ML, Wei Y, Cox-York KA, Gentile CL. Monounsaturated fatty acids protect against palmitate-induced lipoapoptosis in human umbilical vein endothelial cells. PLoS One 2019;14:e0226940.
[11] Peter A, Weigert C, Staiger H, Rittig K, Cegan A, Lutz P, et al. Induction of stearoyl-CoA desaturase protects human arterial endothelial cells against lipotoxicity. Am J Physiol Endocrinol Metab 2008;295:E339–49.
[12] Staiger K, Staiger H, Weigert C, Haas C, Haring HU, Kellerer M. Saturated, but not unsaturated, fatty acids induce apoptosis of human coronary artery endothelial cells via nuclear factor-kappaB activation. Diabetes 2006;55:3121–6.
[13] Listenberger LL, Han X, Lewis SE, Cases S, Farese RV Jr, Ory DS, Schaffer JE. Triglyceride accumulation protects against fatty acid-induced lipotoxicity. Proc Natl Acad Sci U S A 2003;100:3077–82.
[14] Magtanong L, Ko PJ, Dixon SJ. Emerging roles for lipids in non-apoptotic cell death. Cell Death Differ 2016;23:1099–109.
[15] Zheng J, Conrad M. The metabolic underpinnings of ferroptosis. Cell Metab 2020;32:920–37.
[16] Kreuzaler PA, Staniszewska AD, Li W, Omidvar N, Kedjouar B, Turkson J, et al. Stat3 controls lysosomal-mediated cell death in vivo. Nat Cell Biol 2011;13:303–9.
[17] Sargeant TJ, Lloyd-Lewis B, Resemann HK, Ramos-Montoya A, Skepper J, Watson CJ. Stat3 controls cell death during mammary gland involution by regulating uptake of milk fat globules and lysosomal membrane permeabilization. Nat Cell Biol 2014;16:1057–68.
[18] Magtanong L, Ko PJ, To M, Cao JY, Forcina GC, Tarangelo A, et al. Exogenous monounsaturated fatty acids promote a ferroptosis-resistant cell state. Cell Chem Biol 2019;26:420–32 e9.
[19] DeLeve LD, Maretti-Mira AC. Liver sinusoidal endothelial cell: an update. Semin Liver Dis 2017;37:377–87.
[20] Shetty S, Lalor PF, Adams DH. Liver sinusoidal endothelial cells - gatekeepers of hepatic immunity. Nat Rev Gastroenterol Hepatol 2018;15:555–67.
[21] Canali S, Zumbrennen-Bullough KB, Core AB, Wang CY, Nairz M, Bouley R, et al. Endothelial cells produce bone morphogenetic protein 6 required for iron homeostasis in mice. Blood 2017;129:405–14.
[22] Koch PS, Olsavszky V, Ulbrich F, Sticht C, Demory A, Leibing T, et al. Angiocrine Bmp2 signaling in murine liver controls normal iron homeostasis. Blood 2017;129:415–19.
[23] Nedredal GI, Elvevold K, Ytrebo LM, Fuskevag OM, Pettersen I, McCourt PA, et al. Porcine liver sinusoidal endothelial cells contribute significantly to intrahepatic ammonia metabolism. Hepatology 2009;50:900–8.
[24] McMahan RH, Porsche CE, Edwards MG, Rosen HR. Free fatty acids differentially downregulate chemokines in liver sinusoidal endothelial cells: insights into non-alcoholic fatty liver disease. PLoS One 2016;11:e0159217.
[25] Miyao M, Kotani H, Ishida T, Kawai C, Manabe S, Abiru H, et al. Pivotal role of liver sinusoidal endothelial cells in NAFLD/NASH progression. Lab Invest 2015;95:1130–44.
[26] Woudenberg-Vrenken TE, Conde de la Rosa L, Buist-Homan M, Faber KN, Moshage H. Metformin protects rat hepatocytes against bile acid-induced apoptosis. PLoS One 2013;8:e71773.
[27] Choi M, Schreiber A, Eulenberg-Gustavus C, Scheidereit C, Kamps J, Kettritz R. Endothelial NF-kappaB blockade abrogates ANCA-induced GN. J Am Soc Nephrol 2017;28:3191–204.
[28] Geng Y, Hernandez Villanueva A, Oun A, Buist-Homan M, Blokzijl H, et al. Protective effect of metformin against palmitate-induced hepatic cell death. Biochim Biophys Acta Mol Basis Dis 2020;1866:165621.
[29] Geng Y, Wu Z, Buist-Homan M, Blokzijl H, Moshage H. Hesperetin protects against palmitate-induced cellular toxicity via induction of GRP78 in hepatocytes. Toxicol Appl Pharmacol 2020;404:115183.
[30] Verhaag EM, Buist-Homan M, Koehorst M, Groen AK, Moshage H, Faber KN. Hormesis in cholestatic liver disease; preconditioning with low bile acid concentrations protects against bile acid-induced toxicity. PLoS One 2016;11:e0149782.
[31] Qiu B, Simon MC. BODIPY 493/503 staining of neutral lipid droplets for microscopy and quantification by flow cytometry. Bio Protoc 2016;6(17) : e1912.
[32] Drosatos-Tampakaki Z, Drosatos K, Siegelin Y, Gong S, Khan S, Van Dyke T, et al. Palmitic acid and DGAT1 deficiency enhance osteoclastogenesis, while oleic acid-induced triglyceride formation prevents it. J Bone Miner Res 2014;29:1183–95.
[33] Liu L, Shi X, Bharadwaj KG, Ikeda S, Yamashita H, Yagyu H, et al. DGAT1 expression increases heart triglyceride content but ameliorates lipotoxicity. J Biol Chem 2009;284:36312–23.
[34] DeLeve LD, Wang X, Hu L, McCuskey MK, McCuskey RS. Rat liver sinusoidal endothelial cell phenotype is maintained by paracrine and autocrine regulation. Am J Physiol Gastrointest Liver Physiol 2004;287:G757–63.
[35] Vince AR, Hayes MA, Jefferson BJ, Stalker MJ. Sinusoidal endothelial cell and hepatic stellate cell phenotype correlates with stage of fibrosis in chronic liver disease in dogs. J Vet Diagn Invest 2016;28:498–505.
[36] Wang X, Maretti-Mira AC, Wang L, DeLeve LD. Liver-selective MMP-9 inhibition in the rat eliminates ischemia-reperfusion injury and accelerates liver regeneration. Hepatology 2019;69:314–28.
[37] Palomer X, Pizarro-Delgado J, Barroso E, Vazquez-Carrera M. Palmitic and oleic acid: the yin and yang of fatty acids in type 2 diabetes mellitus. Trends Endocrinol Metab 2018;29:178–90.
[38] Peng G, Li L, Liu Y, Pu J, Zhang S, Yu J, et al. Oleate blocks palmitate-induced abnormal lipid distribution, endoplasmic reticulum expansion and stress, and insulin resistance in skeletal muscle. Endocrinology 2011;152:2206–18.
[39] Sargsyan E, Artemenko K, Manukyan L, Bergquist J, Bergsten P. Oleate protects beta-cells from the toxic effect of palmitate by activating pro-survival pathways of the ER stress response. Biochim Biophys Acta 2016;1861:1151–60.
[40] Yasuda M, Tanaka Y, Kume S, Morita Y, Chin-Kanasaki M, Araki H, et al. Fatty acids are novel nutrient factors to regulate mTORC1 lysosomal localization and apoptosis in podocytes. Biochim Biophys Acta 2014;1842:1097–108.
[41] Plotz T, Krummel B, Laporte A, Pingitore A, Persaud SJ, Jorns A, et al. The monounsaturated fatty acid oleate is the major physiological toxic free fatty acid for human beta cells. Nutr Diabetes 2017;7:305.
[42] Plotz T, Hartmann M, Lenzen S, Elsner M. The role of lipid droplet formation in the protection of unsaturated fatty acids against palmitic acid induced lipotoxicity to rat insulin-producing cells. Nutr Metab (Lond) 2016;13:16.
[43] Szafraniec E, Kus E, Wislocka A, Kukla B, Sierka E, Untereiner V, et al. Raman spectroscopy-based insight into lipid droplets presence and contents in liver sinusoidal endothelial cells and hepatocytes. J Biophotonics 2019;12:e201800290.
[44] Chen X, He WT, Hu L, Li J, Fang Y, Wang X, et al. Pyroptosis is driven by non-selective gasdermin-D pore and its morphology is different from MLKL channel-mediated necroptosis. Cell Res 2016;26:1007–20.
[45] Frank D, Vince JE. Pyroptosis versus necroptosis: similarities, differences, and crosstalk. Cell Death Differ 2019;26:99–114.
[46] Zhang Y, Chen X, Gueydan C, Han J. Plasma membrane changes during programmed cell deaths. Cell Res 2018;28:9–21.
[47] Goldberg IJ, Bornfeldt KE. Lipids and the endothelium: bidirectional interactions. Curr Atheroscler Rep 2013;15:365.
[48] Kuo A, Lee MY, Sessa WC. Lipid droplet biogenesis and function in the endothelium. Circ Res 2017;120:1289–97.